Charge density wave in a doped Kondo chain

Yixuan Huang,[1] D. N. Sheng,[2] and C. S. Ting[1,*]

[1]*Texas Center for Superconductivity, University of Houston, Houston, Texas 77204, USA*
[2]*Department of Physics and Astronomy, California State University, Northridge, California 91330, USA*

We report the existence of a charge density wave (CDW) in the ground state of the one-dimensional (1D) Kondo lattice model at the filling of $n = 0.75$ in the weak-coupling region. The CDW is driven by the effective Coulomb repulsion induced by the localized spins. Based on our numerical results using the density matrix renormalization-group method, we show that the CDW phase appears in the paramagnetic region previously known as the Tomonaga-Luttinger liquid. The emergence of this phase serves as an example of a CDW phase induced without bare repulsive interactions, and it enriches the phase diagram of the 1D Kondo lattice model.

I. INTRODUCTION

As a fundamental model for a strongly correlated system describing heavy-fermion materials [1–3] and quantum magnetism [4], the Kondo lattice (KL) model [5–7] has been intensively studied over the past three decades, especially in one dimension [8,9]. While most studies have focused on the Kondo effect and the Ruderman-Kittel-Kasuya-Yosida (RKKY) [10–12] interaction, the effective Coulomb repulsion induced by the localized spins was neglected. In the one-dimensional (1D) bosonization theory, if the interaction is strong enough, the system undergoes a phase transition from the Tomonaga-Luttinger liquid (TLL) to an insulating phase. The TLL phase with a large Fermi surface has been found in the weak coupling [13–15] of the 1D KL model. Whether the effective Coulomb repulsion is strong enough to induce a charge-ordered phase at commensurate filling remains an open question.

The origin of the effective repulsive interaction in a KL model is proposed by a strong-coupling perturbation expansion [16]. However, for 1D the strong-coupling region is dominant by the Kondo effect, which results in ferromagnetism [17,18] at less than half-filling. At half-filling, the insulating phase is caused by the formation of the Kondo singlet, and the Coulomb repulsion is suppressed. The 1D KL model at quarter-filling has also been investigated [19,20] to realize a dimerization of the localized spins induced by the RKKY interaction, although there is some controversy about the existence of true dimer order [21,22]. Thus a charge order may be expected in the next-order commensurate filling of $\frac{1}{8}$ or $\frac{3}{8}$.

The charge order in the KL model has been investigated in higher dimensions. Using the dynamical mean field theory (DMFT) method and the variational Monte Carlo method, a charge density wave in the weak coupling has been found in both two dimensions [23–25] and infinite dimensions [26] at quarter-fillings. The intriguing question remains whether the charge order exists in one dimension, as the DMFT method

generally gets less accurate in low dimensions, especially in one dimension. Additionally, the charge order in higher dimensions is stabilized by the Kondo singlet formation, which is different from the 1D case.

In this work, we identify a charge density wave (CDW) phase at commensurate filling of $\frac{3}{8}$, corresponding to $n = \frac{3}{4}$ in the 1D KL model, as shown in Fig. 1. The phase is characterized by a finite density oscillation in an arbitrarily long chain, and a vanishing Luttinger parameter. The formation of the CDW opens a gap in the charge sector, similar to the metal-insulator transition in the 1D extended Hubbard model [27,28], while the spin part remains gapless. Our results showing the charge-ordered phase in 1D at higher-order commensurate filling provide an insight into the exotic phase of the KL model, and a possible mechanism of the charge order in 1D organic compounds [29,30], especially the Peierls instabilities of D_2X salt, where D is a fluoranthene or perylene derivative and X is AsF_6 or PF_6 [31,32]. Besides, a direct test of our results could be made through the experimental laboratory of ultracold atoms [33], or an artificial 1D KL by precise ion beam irradiation of a 1D quantum wire [34]. In the existence of a CDW, the behavior of the localized spin is the result of the competition between RKKY interaction and CDW, which provides an example of how the CDW interacts with the localized spins.

II. MODEL AND METHODS

In this work, we consider the standard one-dimensional Kondo lattice (KL) model, which describes the itinerant electrons coupled to the localized spins on every unit with a SU(2) symmetric antiferromagnetic interaction:

$$\mathcal{H} = -t \sum_{i=1,\sigma}^{L-1} c_{i,\sigma}^{\dagger} c_{i+1,\sigma} + \text{H.c.} + J \sum_{i=1,\sigma}^{L} \vec{S}_i \cdot \vec{s}_i. \quad (1)$$

The first term in the Hamiltonian is the hopping term, where $c_{i,\sigma}^{\dagger}$ refers to the creation operator of an electron on site i with spin index σ, the second term describes the spin-spin interaction where $\vec{S}_i$ denotes the localized spin-$\frac{1}{2}$,
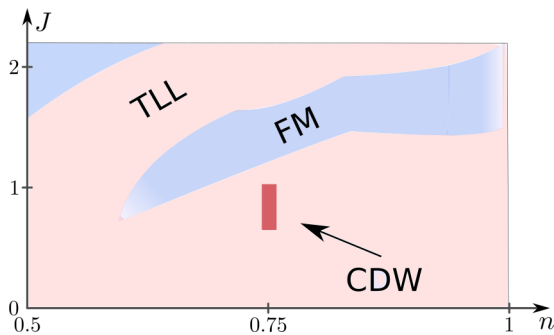
FIG. 1. A schematic diagram of the 1D Kondo lattice model in the region of $n > 0.5$ and $J < 2.2$, where n is the electron density and J is the coupling between electrons and localized spins.

and $\vec{s_i} = \frac{1}{2} \sum_{\alpha,\beta} c_{i,\alpha}^{\dagger} \vec{\sigma}_{\alpha,\beta} c_{i,\beta}$ (with Pauli matrices $\vec{\sigma}$) is the conduction electron spin.

The strong correlations in the weak coupling between electrons and localized spins makes it notoriously difficult for exact solutions. Thus the numerical method becomes important in order to determine the phase diagram.

We use the U(1) density matrix renormalization group [35–37] (DMRG) method with an open boundary condition for lattice sizes up to $L = 208$. Calculations are performed using the ITensor library [38]. Smaller sizes are also used for finite-size extrapolation. The largest bond dimension is 7000 during the sweeps. A total of 140 sweeps with increasing bond dimension were used in order to reach a stable and convergent ground state. The cutoff error during the last few sweeps is 10^{-7}. The hopping parameter t and the lattice spacing are set to unity to fix the energy scale.

III. CDW ORDER AT $n = \frac{3}{4}$

Under the open boundary condition, the electron density in the CDW phase shows a modulation in real space as a result of spontaneous symmetry breaking. While the Mermin-Wagner theorem [39] forbids any spontaneous breaking of continuous symmetry in 1D, the CDW only breaks the lattice translational symmetry, which is discrete. In Fig. 2(a) we show $\langle N_i \rangle$ at $J = 0.9$ and $L = 160$. There are strong oscillations around the average electron density with the amplitude ≈ 0.03. The oscillation decays very slowly away from the boundary and remains finite in the middle of the chain. This allows us to define the order parameter as $A = \lim_{L \to \infty} A(L/2)$, which is the amplitude of electron density oscillation in the middle.

The finite-size extrapolation is needed to determine the order parameter in the large system limit. The extrapolated order parameter is plotted against J in Fig. 2(c). When J is close to the critical point slightly above 1.0, the order parameter quickly rises from 0, and then it decreases slowly to 0 as J decreases. Figure 2(d) shows the finite-size extrapolation of the order parameter for various couplings. Inside the parameter range from $J = 0.7$ to 1.0, $A(L/2)$ has a weak dependence of L, and it remains a finite value as L goes to infinity.

The Fourier transform of the electron density in Fig. 2(a) is plotted in Fig. 2(b). We have used the smoothed Fourier transform in order to minimize the effect caused by the open
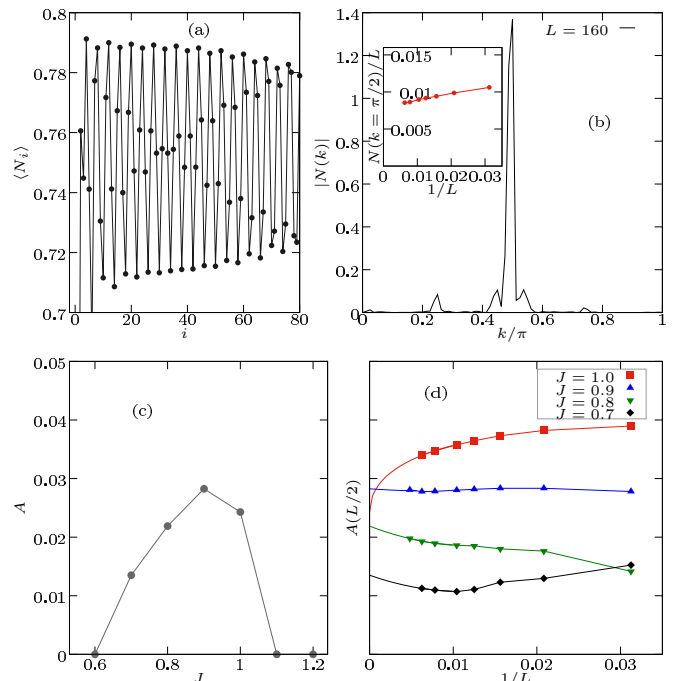

FIG. 2. Part (a) is the electron density at $J = 0.9$, $L = 160$, and $n = \frac{3}{4}$. Only half of the lattice is shown. Part (b) is the Fourier transform of the density oscillation in (a). The dominant peak shows up at $k = \frac{\pi}{2}$. The inset of (b) shows the intensity of the $k = \frac{\pi}{2}$ peak divided by the length. Part (c) is the J dependence of the oscillation amplitude in the middle after finite-size extrapolation. The extrapolation in (d) is conducted in this way. If the fitting agrees well with the power decay of the Friedel oscillation [13] in TLL, then the order parameter is considered zero when $L \to \infty$ (see the Supplemental Material [40]), otherwise we use a least-squares fit to the second order of polynomials in $1/L$. For J close to the transition, we find it better to fit to $1/\sqrt{L}$ as the similar scaling in TLL.

boundary. The details of the window function that we use are discussed in Refs. [41,42]. Here the CDW phase is dominant by a single peak at $k = \frac{\pi}{2}$, which corresponds to the oscillation period of four lattice spacings. There may be a superposition of another oscillation frequency such as $k = \frac{\pi}{4}$, but they all vanish in the thermodynamic limit as illustrated later. The inset of Fig. 2(b) shows the intensity of the dominant peak divided by the lattice size. The intensity has an almost linear dependence on L and remains finite after the extrapolation.

The structure factor $N(k)$ of the charge-ordered phase always scales as the order parameter multiplied by the lattice length. In the infinite chain limit, the order parameter defined by the structure factor is essentially equivalent to the definition of the oscillation amplitude in the middle of the chain. As shown in Fig. 2(d) and the inset of Fig. 2(b), the order parameters both remain finite in the CDW phase.

The Luttinger parameter k_L in the TLL of the 1D KL model shows a monotonic decrease as J decreases at the fixed electron density [14,15], indicating a strong repulsive interaction between electrons in the weak-coupling region. This could explain the formation of a CDW under strong repulsion. However, in the limit of $J \to 0$, the system goes back to free 1D electrons with $k_L = 1$. Thus it is natural to see
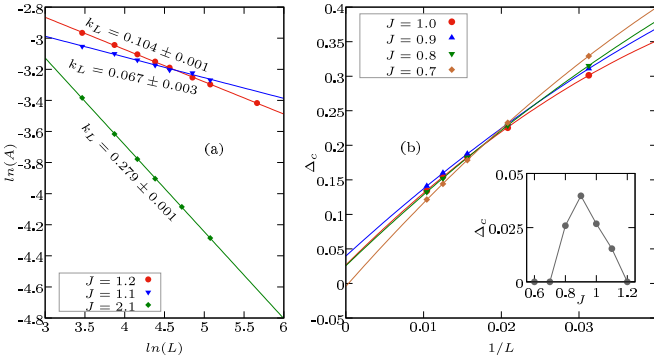
FIG. 3. Part (a) is the log-log plot of the Friedel oscillation amplitude in the middle of various lengths. The Luttinger parameter k_L is determined by the slope $= -2k_L$. The error of k_L is given by the standard deviation of the least-squares fit. The Luttinger parameter decreases as we lower J into the weak-coupling region, which agrees with previous papers. For $J = 1$ it cannot be linearly fit, indicating the onset of CDW. Part (b) is the finite-size extrapolation of the charge gap at $n = \frac{3}{4}$. Four examples of J are given for the least-squares fit. The inset of (b) shows the extrapolated charge gap for various J.

a critical point where the effective repulsive interaction is not strong enough to stabilize CDW, and the system goes back to TLL. In the bosonization picture, the umklapp-type scattering term, which carries a fast oscillation phase factor, only appears in the low-energy effective Hamiltonian at special fillings [43],

$$\Psi_{R,\uparrow}^{\dagger} \Psi_{R,\downarrow}^{\dagger} \Psi_{L,\uparrow} \Psi_{L,\downarrow} \propto e^{-i4K_F x} e^{i2\sqrt{2}\phi_\rho(x)}. \tag{2}$$

If $4K_F = 2\pi$, corresponding to $n = 1$, the fast oscillation term becomes constant in Eq. (2) and enters in the low-energy effective Hamiltonian. If $k_L < 1$, then this term is relevant in the renormalization procedure, and it opens a gap in the charge sector. Higher-order terms of umklapp scattering could also occur at other commensurate fillings. In our case of $n = \frac{3}{4}$, the fourth power term of the umklapp scattering can occur in the extremely small value of $k_L < \frac{1}{16}$. In fact, as we vary J at $n = \frac{3}{4}$, $k_L \to \frac{1}{16}$ when the system is close to the phase transition.

To determine the Luttinger parameter in the TLL phase, we compare the Friedel oscillation [13] amplitude at the center for different lattice sizes. The methods that we used to determine the Luttinger parameter are adopted from Ref. [42]. As shown in Fig. 3(a), we fit the log-log plot of the oscillation amplitude and find that for $J = 1.1$ the Luttinger parameter is 0.067, which is very close to the critical value of $\frac{1}{16}$. This agrees with the assumption that the CDW is driven by the strong effective Coulomb repulsion. Near the critical J, the oscillation decay rate is so slow that we cannot be sure whether the oscillation will vanish in the limit of an infinitely long chain [42]. Although it is hard to determine the exact critical value of J, the Luttinger parameter close to the transition point provides additional evidence of the emergence of the CDW.

Now we investigate the charge gap in the CDW. Figure 3(b) shows the J dependence of the charge gap at $n = \frac{3}{4}$, which is

defined as

$$\Delta_c = \lim_{L \to \infty}[E_0(N_e = N + 2)$$
$$+ E_0(N_e = N - 2) - 2E_0(N_e = N)], \tag{3}$$

where the $E_0(N_e)$ refers to the ground-state energy of a given electron number. Here we set $N = \frac{3}{4}L$ to fix the electron density. We choose J carefully to avoid the ferromagnetic region so that the ground state is always in the $S_z^{\text{tot}} = 0$ subspace. The charge gaps here only depend on the ground-state energy calculated by the DMRG method, thus they are very reliable. In Fig. 3(b), the charge gap is extrapolated by a least-squares fit to the second order of polynomials in $1/L$. A nonzero value of the gap can be distinguished in the thermodynamic limit. The inset of Fig. 3(b) shows the extrapolated result of the charge gap at different values of J. The gap reaches a maximum value at around $J = 0.9$, and it decreases monotonically to 0 apart from the peak. Generally in a gapped phase the correlation function either has an exponential decay or it decays to a constant at large separations. The electron density oscillation agrees with the latter case here. The emergence of a nonzero charge gap is consistent with the CDW, and together with the CDW order parameter, we can establish the TLL-CDW phase boundary at $J \approx 1.1$ and 0.7.

The measurement of the Zeeman field needed to close the charge gap could be used as a scale of finite transition temperature $T_c \sim \frac{\mu_B h_c}{k}$. We found $h_c = 0.03$ at $J = 0.9$, where the CDW is also destroyed.

The spin gap is defined in a similar way, $\Delta_s = E_0(S_z^{\text{tot}} = 1) - E_0(S_z^{\text{tot}} = 0)$, except that $E_0(S_z^{\text{tot}} = -1)$ is not needed due to the spin symmetry. We have calculated the spin gaps for several J with different lattice sizes, and the gap is always zero with an error bar in the order of the truncation error. Although numerically we can never rule out a very tiny spin gap in larger sizes, additional evidence to support the vanishing spin gap is found considering the density oscillation period. The effective spin in one unit cell remains a half-integer number, which resembles the spin-half Heisenberg model with gapless spin excitation.

IV. CORRELATIONS

We then turn to the correlation of the localized spins in the CDW. Unlike the charge part, the total spin of the ground state preserves the SU(2) symmetry (see the Supplemental Material [40]). The RKKY interaction between the localized spins could lead to a possible valence bond solid, as was reported in the 1D KL at quarter-filling [19].

We first investigate the nearest-neighbor correlation of the localized spins, i.e., $\langle S_i S_{i+1} \rangle$. Figure 4(a) shows that the correlation has $k = \frac{\pi}{2}$ oscillations with a superposition of incommensurate oscillations with $k = \frac{\pi}{L}$, which is size-dependent. Generally in a valence bond solid, the dimer order described by the short-ranged spin correlation should be L-independent away from the boundary, as in the example of the KL model on the zigzag ladder at half-filling [44]. Quantum fluctuations will destroy any incommensurate order in 1D, so the leading order at the weak coupling of $n = \frac{3}{4}$ is just the charge order. The average correlation of the nearest-neighbor spins is antiferromagnetic, which is consistent with the RKKY interaction
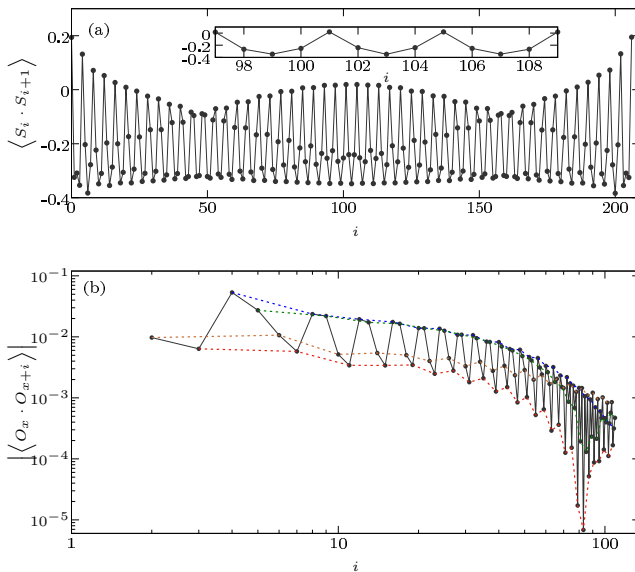
FIG. 4. The nearest-neighbor (a) and long-range dimer-dimer (b) correlation of the localized spins at $J = 0.9$, $L = 208$, and $n = \frac{3}{4}$. In (a) the average correlation is around -2.0, which is L-independent. The incommensurate oscillation refers to the upper bound in the middle with $k = \frac{\pi}{L}$. The amplitude of the incommensurate oscillations has almost no dependence of the lattice length. The inset of (a) shows the dominant oscillation of the correlation with a period of 4, which is the same period as the CDW. In (b) we calculate the correlation at $x = 29$ to minimize the boundary effect. The plot uses a logarithmic scale on both axes in order to identify the decay mode. The dimer-dimer correlation also has an oscillation period of 4. The four colored dashed lines are merely the correlation of every four points connected, because they each have a different pattern. The correlation functions of the TLL are not shown here as they have monotonic power-law decays, which agrees with the bosonization theory.

close to half-filling. Here the correlation of the localized spins cannot be explained by the low-energy effective Heisenberg model with RKKY couplings because of the existence of charge fluctuations. We believe the $k = \frac{\pi}{2}$ oscillation of the localized spin correlation is mainly induced by the $k = \frac{\pi}{2}$ CDW because of the antiferromagnetic coupling between the electron spins and the localized spins.

For further illustration, we study the dimer-dimer correlations, which are defined as the two-point correlation functions of the localized spins $\langle O_x O_{x+i} \rangle$, where $O_x = S_x S_{x+1}$ refers to the nearest-neighbor spin correlation. The $\langle O_x O_{x+i} \rangle$ plotted in Fig. 4(b) shows a decay over distance, although in an

oscillation fashion. The correlation is dominant by the blue line, indicating a slow exponential decay. This is different from the TLL where correlation functions generally have power-law decays. It seems that the correlation saturates toward a finite value for the green and red line at around $i = 80$, but after analyzing the dimer-dimer correlation at different points, we find that it always "saturates" near the middle of the lattice. The similar "saturation" is also found in the TLL phase at $J = 2.1$ and $n = \frac{3}{4}$. We argue that this is just an artificial effect due to the finite size of system, as the correlation will have a monotonic decay in the limit of an infinite chain. This is consistent with our conclusion that the phase at $n = \frac{3}{4}$ for weak J is dominant by the charge order.

V. CONCLUSIONS

We have used the DMRG method to obtain the ground state of the 1D KL model and provide compelling evidence for CDW at $n = \frac{3}{4}$; a similar CDW is not found at the other commensurate filling of $n = \frac{1}{4}$ (see the Supplemental Material [40]). Our numerical results are consistent with the bosonization prediction near the phase transition, suggesting that the CDW is driven by the effective Coulomb repulsion, which is qualitatively different from the CDW in higher dimensions [23,26], and at extremely small J in 1D predicted recently [45]. We also find that the CDW is insulating, while the phase at incommensurate filling or generally in TLL is metallic. Under the existence of the CDW, the localized spin has formed a similar oscillation pattern, while preserving the total spin SU(2) symmetry. Other magnetic orders such as the antiferromagnetic order have not been found in the CDW phase. Our results provide a simple mechanism of the charge order in 1D organic compounds. The emergence of the CDW may have implications for the novel phase diagram of the KL model in higher dimensions.

[1] Z. Hossain, M. Schmidt, W. Schnelle, H. S. Jeevan, C. Geibel, S. Ramakrishnan, J. A. Mydosh, and Y. Grin, Phys. Rev. B **71**, 060406(R) (2005).

[2] A. Ochiai, T. Suzuki, and T. Kasuya, J. Phys. Soc. Jpn. **59**, 4129 (1990).

[3] L. Wang, Z. Fu, J. Sun, M. Liu, W. Yi, C. Yi, Y. Luo, Y. Dai, G. Liu, Y. Matsushita *et al.*, npj Quantum Mater. **2**, 36 (2017).

[4] G. R. Stewart, Rev. Mod. Phys. **73**, 797 (2001).

[5] S. Doniach, Physica B+C **91**, 231 (1977).

[6] C. Lacroix and M. Cyrot, Phys. Rev. B **20**, 1969 (1979).

[7] P. Fazekas and E. Müller-Hartmann, Z. Phys. B **85**, 285 (1991).

[8] H. Tsunetsugu, M. Sigrist, and K. Ueda, Phys. Rev. B **47**, 8345 (1993).

[9] H. Tsunetsugu, M. Sigrist, and K. Ueda, Rev. Mod. Phys. **69**, 809 (1997).

[10] M. A. Ruderman and C. Kittel, Phys. Rev. **96**, 99 (1954).

[11] T. Kasuya, Prog. Theor. Phys. **16**, 45 (1956).

[12] K. Yosida, Phys. Rev. **106**, 893 (1957).

[13] N. Shibata, K. Ueda, T. Nishino, and C. Ishii, Phys. Rev. B **54**, 13495 (1996).

[14] N. Shibata, A. Tsvelik, and K. Ueda, Phys. Rev. B **56**, 330 (1997).

[15] I. Khait, P. Azaria, C. Hubig, U. Schollwöck, and A. Auerbach, Proc. Natl. Acad. Sci. USA **115**, 5140 (2018).

[16] J. E. Hirsch, Phys. Rev. B **30**, 5383 (1984).

[17] I. P. McCulloch, A. Juozapavicius, A. Rosengren, and M. Gulacsi, Phys. Rev. B **65**, 052410 (2002).

[18] R. Peters and N. Kawakami, Phys. Rev. B **86**, 165107 (2012).

[19] J. C. Xavier, R. G. Pereira, E. Miranda, and I. Affleck, Phys. Rev. Lett. **90**, 247204 (2003).

[20] J. C. Xavier and E. Miranda, Phys. Rev. B **78**, 144406 (2008).

[21] C. Hotta and N. Shibata, Physica B **378**, 1039 (2006).

[22] N. Shibata and C. Hotta, Phys. Rev. B **84**, 115116 (2011).

[23] T. Misawa, J. Yoshitake, and Y. Motome, Phys. Rev. Lett. **110**, 246401 (2013).

[24] Y. Motome, K. Nakamikawa, Y. Yamaji, and M. Udagawa, Phys. Rev. Lett. **105**, 036403 (2010).

[25] T. Sato, F. F. Assaad, and T. Grover, Phys. Rev. Lett. **120**, 107201 (2018).

[26] R. Peters, S. Hoshino, N. Kawakami, J. Otsuki, and Y. Kuramoto, Phys. Rev. B **87**, 165133 (2013).

[27] E. Jeckelmann, Phys. Rev. Lett. **89**, 236401 (2002).

[28] A. W. Sandvik, L. Balents, and D. K. Campbell, Phys. Rev. Lett. **92**, 236401 (2004).

[29] H. Seo, C. Hotta, and H. Fukuyama, Chem. Rev. **104**, 5005 (2004).

[30] P. Monceau, Adv. Phys. **61**, 325 (2012).

[31] V. Ilakovac, S. Ravy, A. Moradpour, L. Firlej, and P. Bernier, Phys. Rev. B **52**, 4108 (1995).

[32] J.-P. Pouget, P. Foury-Leylekian, and M. Almeida, Magnetochemistry **3**, 13 (2017).

[33] L. Riegger, N. Darkwah Oppong, M. Höfer, D. R. Fernandes, I. Bloch, and S. Fölling, Phys. Rev. Lett. **120**, 143601 (2018).

[34] L. Pfeiffer, H. Störmer, K. Baldwin, K. West, A. Goni, A. Pinczuk, R. Ashoori, M. Dignam, and W. Wegscheider, J. Cryst. Growth **127**, 849 (1993).

[35] S. R. White, Phys. Rev. Lett. **69**, 2863 (1992).

[36] S. R. White, Phys. Rev. B **48**, 10345 (1993).

[37] U. Schollwöck, Ann. Phys. **326**, 96 (2011).

[38] http://itensor.org/.

[39] N. D. Mermin and H. Wagner, Phys. Rev. Lett. **17**, 1133 (1966).

[40] See Supplemental Material at http://link.aps.org/supplemental/10.1103/PhysRevB.99.195109 for detailed numerical results.

[41] M. Vekić and S. R. White, Phys. Rev. Lett. **71**, 4283 (1993).

[42] S. R. White, I. Affleck, and D. J. Scalapino, Phys. Rev. B **65**, 165122 (2002).

[43] T. Giamarchi, *Quantum Physics in One Dimension* (Oxford University Press, Oxford, 2004), Vol. 121.

[44] M. Peschke, R. Rausch, and M. Potthoff, Phys. Rev. B **97**, 115124 (2018).

[45] A. Tsvelik and O. Yevtushenko, arXiv:1812.11507.